Published in Conference Record of the 23th IEEE Photovoltaic Specialists Conference, 878-884, 1993
which should be used for any reference to this work

AMORPHOUS SILICON SOLAR CELLS WITH GRADED LOW-LEVEL DOPED i-LAYERS CHARACTERISED BY BIFACIAL MEASUREMENTS

D. Fischer, N. Wyrsch, C. M. Fortmann, A. V. Shah,
Institute of Microtechnology, University of Neuchâtel,
Breguet 2, 2000 Neuchâtel, Switzerland,
phone +41 38 20 51 21, fax +41 38 25 42 76

ABSTRACT

Bi-facial spectral response characterization of solar cells under near operating condition illumination is used in conjuncture with a novel bi-facial DICE analysis to establish the collection efficiency as a function of i-layer position in p-i-n amorphous silicon solar cells. A significant portion of solar cell degradation can be explained in terms of electric field distortions which increase recombination losses. Unlike carrier lifetime reductions the field distortions can be reduced. The numerical model is used to guide the intentional doping of the i-layer to counteract the field distortions caused by charged dangling bonds, and thus to optimize the electric field for the degraded state. Solar cells with graded low-level boron doping in the i-layer are analysed in detail. Increasing conversion efficiency during light-soaking, and enhanced stabilized n-side performance show the viability of the electric field optimization.

INTRODUCTION

Many changes occur in the i-layer of p-i-n amorphous silicon solar cells due to light exposure. The most significant of which is a reduction in carrier lifetime due to an increase in the density of dangling bond defects. Despite an intense effort by the amorphous silicon research community there appears to be no effective means by which to reduce the defect generation rate to an acceptable level for the preparation of efficient, thick i-layer solar cells.

Presently the most promising means by which more stable amorphous silicon based solar cells will be prepared is the multi-junction solar cell. These devices use a number of solar cells each with an i-layer as thin as possible in order to provide electric fields strong enough to overcome the loss in carrier lifetime caused by degradation. The i-layers of the stacked solar cells become progressively thicker because the bottom solar cells must current match to the top cell using the more weakly absorbed red portion of the solar spectrum. For this reason it is the bottom cells that limit the stable efficiency of these multi-junction devices.

While in the not-too-distance past all the solar cell degradation would have been attributed to changes in carrier lifetime caused by defect related recombination it is becoming increasingly apparent that some of the problems associated with degradation are related to the nature of the charge states available to these defects. These charged defects distort the electric field and lessen its ability to extract the photo-generated carriers particularly in the degraded state [1]. Ultimately it is the field distortions that set the maximum i-layer thickness for stable solar cell performance.

Unlike the defect generation problem itself which appears to have no solution (at present) there is a real possibility to compensate the electric field distortions caused by the light induced defects through the use of low level impurity doping in the i-layer [2]. This work will explore the entire issue of field distortions caused by charged light induced defects and their solution. In order to accomplish this task new methods of solar cell characterization, analysis, and preparation had to be developed:

- bi-facial spectral response measurement with operating condition bias illumination
- DICE analysis of bifacial spectral response to obtain collection probability as a function of i-layer position
- numerical modelling of p-i-n solar cells to estimate the charged defect distributions, and to evaluate the potential of electric field optimisation
- fabrication of solar cells with intentionally distorted electric fields to verify modelling and analysis techniques
- develop methods to determine the density of active dopants in the solar cell
- fabrication of proof-of-concept solar cells in which the effect of charged light induced defects was compensated by low level impurity doping

METHODS

The a-Si:H solar cells were deposited by plasma-enhanced glow discharge at 70 MHz in a single chamber reactor with load-lock. The following solar cell structures were deposited on textured TCO coated substrates at a substrate temperature of 220°C: 120 Å p^+a-Si:C:H / 5000 Å a-Si:H / 300 Å $n^+\mu$c-Si:H. A 1200 Å thick layer of ITO was employed to provide transparent back contact. For the graded low-level doping studies parts of the i-layer were intentionally doped with boron. Doping concentrations throughout the paper refer to the gas phase concentrations (vppm) of diborane (B_2H_6) diluted by silane (SiH_4).

Light-soaking of the solar cells was performed under illumination from a sodium vapor discharge lamp. The light intensity was adjusted to yield the same short circuit current as 100 mW/cm^2 AM1.5.

The bifacial characterisation included J-V measurement by a double source Wacom solar simulator under 100 mW/cm^2 AM1.5 illumination, and under AM1.5 light filtered by a RG610 low-pass filter (transmission onset at 610 nm) to simulate the illumination spectrum incident on the second cell of a multi-junction device.

Also, p-side and n-side small signal quantum efficiencies (QE) were measured, with and without bias light, and as a function of bias voltage. The QE data was also de-convoluted by the bifacial DICE (dynamic inner collection efficiency) method [3] to determine the collection as a function of the i-layer depth. This analysis method is based on the original DICE method introduced by Takahama [4]. By employing p-side and n-side QE to extract one single set of DICE values, the errors of the original method for the regions far from the illuminated (typically p-side) surface are significantly reduced, leading to a more accurate collection profile.

The electric field in the p-i-n cells was determined by the transient charge collection efficiency method [5]. This method

has been successfully applied to determine the electric field profiles in degraded p-i-n solar cells [6]. The main limitation of this method is that it is only valid in the regions of the device where the second derivative of the electric field stays permanently < 0. This means that regions with increasing electric field can not be measured. Additionally, the results can be influenced by incomplete charge collection, caused by deep trapping of the carriers. However, even with deep trapping the measured electric field profile will still represent a lower bound to the actual profile.

P-I-N SOLAR CELLS WITHOUT i-LAYER DOPING

First, the influence of light-soaking on standard p-i-n solar cells (no low-level doping) is analysed. Figure 1 shows the IV curves for different illumination conditions of a 0.5 µm thick solar cell as a function of light-soaking time. In the annealed state, high collection is found under forward bias voltage (for all illumination conditions), with fill factors of ~0.65. With increasing light-soaking time the forward bias currents drop continually, while the reverse bias currents tend to stay constant. The decay at forward bias is found to strongly depend on the type of illumination incident during the measurement: for p-side AM1.5 illumination, a relatively small current collection reduction is observed, for the red light illumination, a larger decay is observed, and for n-side AM1.5 illumination, a much stronger decay of the current collection is noted. Table I shows the corresponding efficiency data: For p-side AM1.5 illumination, a relative conversion efficiency degradation of 30% is found, compared to 60% degradation for n-side AM1.5 illumination. This is in agreement with stability investigations conducted over 10 years ago [7], when p-i-n where found to be more stable than n-i-p devices.

Table I: Effect of the degradation for different generation profiles in a 0.5 µm p-i-n solar cell

illumination	$\eta_{annealed}$ [%]	η_{450h} [%]	$\eta_{450}/\eta_{annealed}$
p-side AM1.5	7.63	5.35	0.70
p-side red light *)	2.44	1.37	0.56
n-side AM1.5	5.98	2.40	0.40

*): AM1.5 filtered with RG610 filter

Figure 2 shows p- and n-side QE in the annealed state, and after 425 h of light-soaking. In the annealed state, p- and n-side QE stay closed to the optical envelope over the whole wavelength range. After the light-soaking, the p-side QE stays high for short wavelengths, whereas some decay is found in the long wavelength range, in agreement with other investigations [8,9]. The n-side QE shows a large drop in the short wavelength range and a smaller drop in the long wavelength range (the long wavelength collection must be the same for both p- and n-side illumination !).

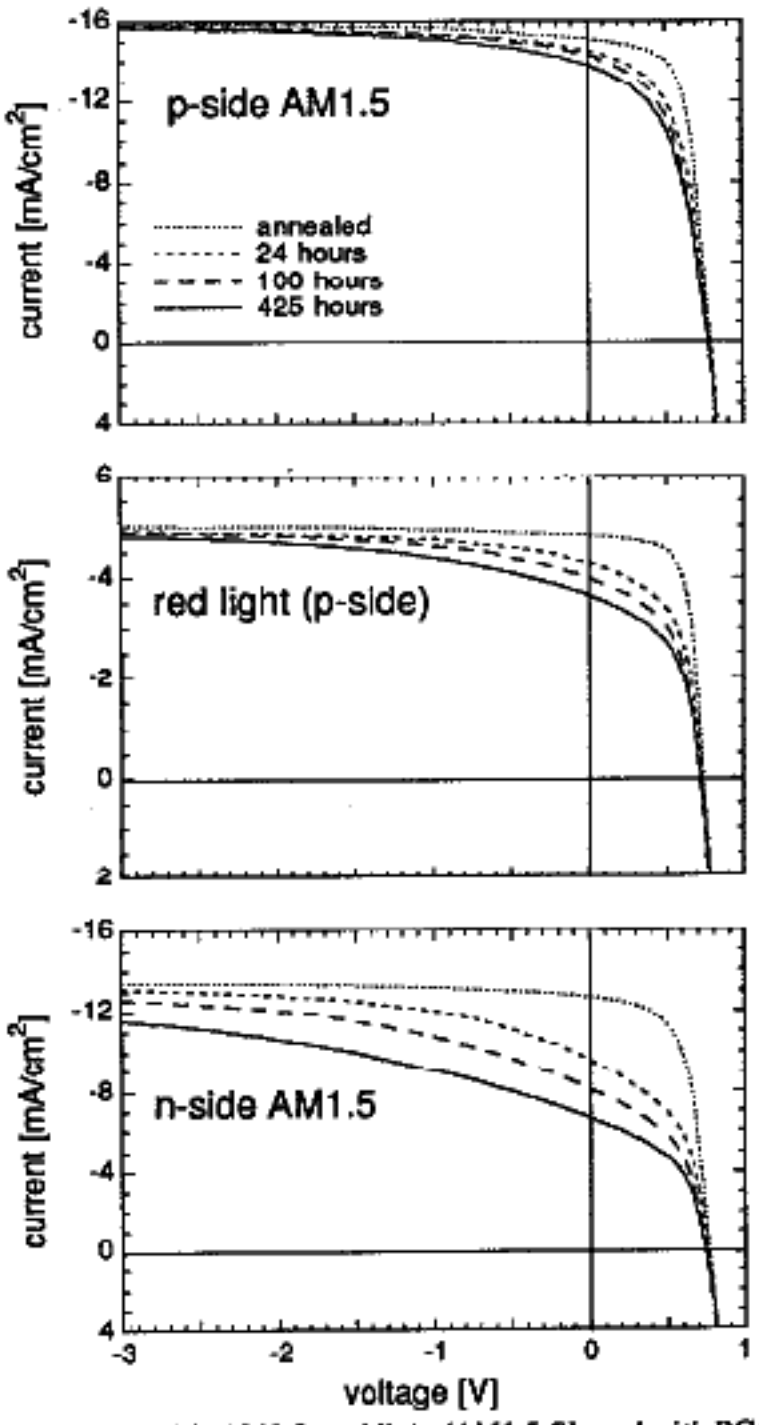

Figure 1: p-side AM1.5, red light (AM1.5 filtered with RG610 low-pass filter), and n-side AM1.5 IV curves of a p-i-n solar cell with undoped i-layer, in the annealed state and for different times of light-soaking (i-layer thickness 0.5 µm).

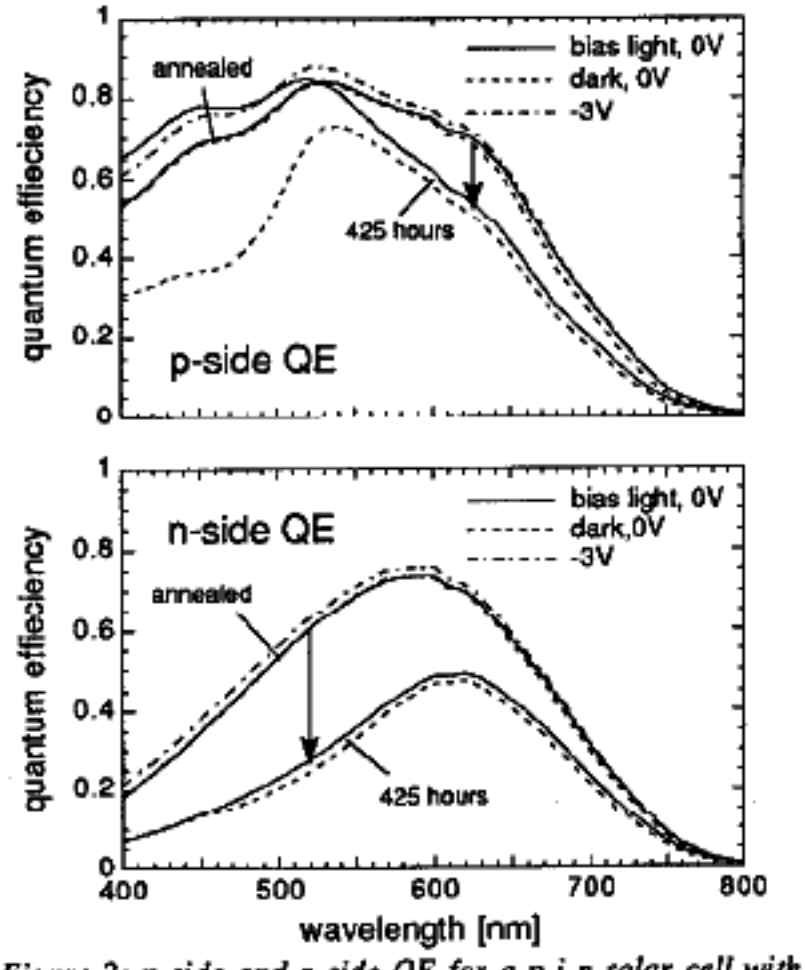

Figure 2: p-side and n-side QE for a p-i-n solar cell with undoped i layer in the annealed state and after 425 hours of light-soaking, measured with and without red bias light (i-layer thickness 0.5 µm).

Table II: Effect of the bias-light on the integrated QE

sample status	Isc mA/cm^2	$\int QE_{biaslight}$ mA/cm^2	$\int QE_{dark}$ mA/cm^2
annealed	14.6	14.4	14.0
24 hours	14.4	14.2	12.0
425 hours	13.6	13.5	10.1

The QE measurements as discussed refer to those measured under bias light illumination (red light with the intensity of about one sun was used). The considerable discrepancy between QE with and without bias light in the short wavelength range for p-illumination (Figure 2 top) has led to considerable controversy in the past. It has been argued that the bias light could be hiding degradation effects in the short wavelength region [8]. But recently it has been shown that the drop in dark QE is due to a strong electric field distortion, if the back of a degraded cell is not bias light illuminated (electron self blocking)[10]. Thus this effect is by no means representative of the actual collection of the short wavelength light in the operating solar cell (the observed short wavelength drop without bias light can, however, be a useful tool to characterize the i-layer defect density in a solar cell [11]). Only by applying the bias light, the solar cell is placed in the actual operating conditions, and the measured collection is representative of the actual performance of the solar cell. This is confirmed by the integrated QE currents, which show a good agreement with the measured currents (JV) only if the bias light QE is used (Table II). Also, the comparison of the voltage dependent QE of red light to the IV of red light shows excellent agreement (Figure 3). In summary the analysis of QE data acquired under bias light shows not only good qualitative agreement, but also quantitative correspondence to JV data of p-i-n solar cells.

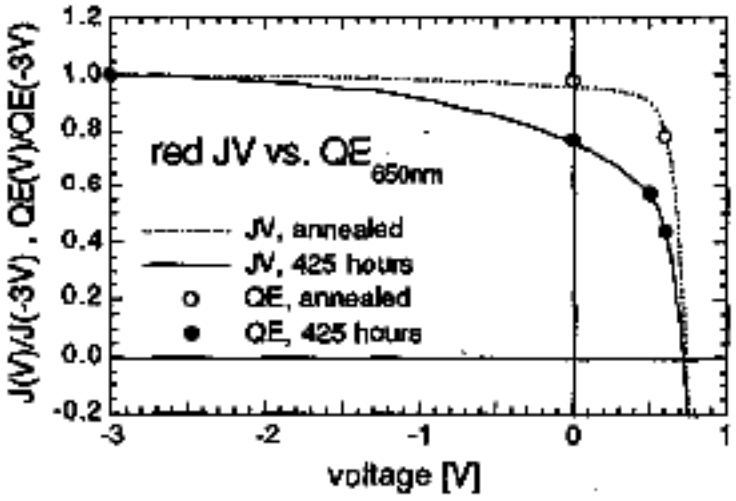

Figure 3: Comparison of the red light (AM1.5 filtered with RG610) current collection and the voltage dependent QE at 650 nm in a 0.5 µm, undoped p-i-n solar cell (annealed and after 425 hours of light-soaking).

Bias light p- and n-side QE data was used as input for bifacial DICE analysis. Figure 4 shows the collection profiles at 0 V as a function of light-soaking time. In the annealed state, high collection probability found across the entire i-layer. After light-soaking, a systematic decrease of the collection probability is seen towards the n-side: While at the p-i interface the collection probability remains close to 100 %, the collection at the n-i interface is reduced to as low as ~30 % after 425 hours of light-soaking. This collection pattern is consistent with the JV measurements (Figure 1): Given the highly non-uniform generation profile of the AM1.5 light (~50 % of the carriers are generated within the 800 Å below the illuminated surface), p-side AM1.5 light conversion shows a relative insensitivity to the light-soaking, and n-side AM1.5 light conversion exhibits strong reduction as most of the generation occurs in the region most affected by the light-soaking.

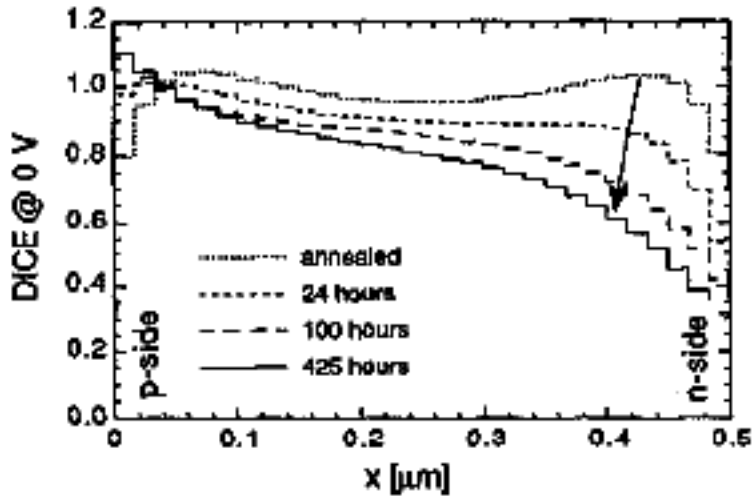

Figure 4: Bifacial DICE profiles at 0 V of an undoped p-i-n solar cell (0.5 µm) in the annealed state and for different times of light-soaking. The QE data was measured under red bias light and normalized with respect to the QE at -3 V.

The asymmetric collection in light-soaked solar cells can be understood by a two step reasoning. First, the creation of mid-gap defects in numbers >10^{16} cm^{-3} by the light-soaking leads to a significant distortion of the electric field in the i-layer. As previously described [1], the defects tend to charge positively towards the p-side, and negatively towards the n-side, yielding high fields towards the interfaces, and a low field in the bulk. This view can explain the drop of the collection from the p-side towards the bulk, but towards the n-side, the collection would be expected to raise again due a high field at the n-i interface. Secondly, the asymmetry seen in the measurements can be understood as the effect of an asymmetry in defect charging that arises from the difference in the carrier mobilities of holes and electrons. Since both carriers must support the same photo-current, the bulk hole concentration must on average be higher than that of the electrons. This results in a larger positive space charge at the p-side as compared to the corresponding negative charge at the n-side. This general behavior was detected by numerical modelling of degraded solar cells [3]. In these modelling results, which yielded good agreement with measured QE data, the asymmetric space charge lead to significant electric field increase at the p-i interface in the degraded state, and a corresponding electric field reduction in the back half of the i-layer. No electric field increase due to charged defects was found at the n-i interface.

In the past, often the asymmetry of the collection has been explained in terms of hole limited transport [e.g. 7]. As explained above, the asymmetry is in fact rooted in the difference in carrier mobility, but in an indirect way by influencing the overall electric field distribution in the i-layer. The local hole lifetime in the solar cell itself is a strong function of the charge state of the defects, and therefore of the position in the i-layer. In the bulk of the i-layer, the excess hole lifetime is actually higher than that of the electrons, as the concentration of holes is higher, and the electron and hole recombination rates are equal.

P-I-N SOLAR CELLS WITH GRADED LOW-LEVEL BORON DOPING

The asymmetric electric field distortion component of solar cell degradation can be addressed by optimizing the electric field distribution through graded impurity doping of the i-layer, as proposed by independent researchers [2]. The

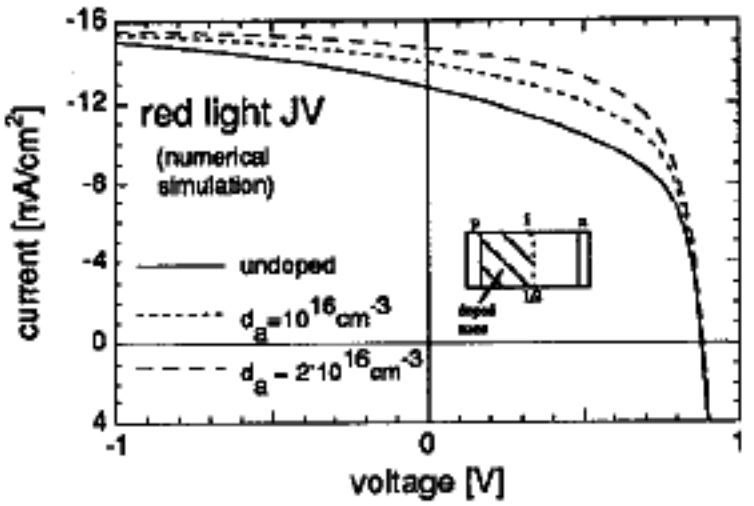

Figure 5: Numerically simulated degraded state red light JV for p-i-n solar cells (0.5 μm) with and without graded acceptor profiles in the i layer. (d_a=acceptor concentration). The density of amphoteric midgap defects is $3\cdot10^{16}cm^{-3}$. The other modelling parameters are described elsewhere [3,11].

possibility of a gain in single junction solar cells appears to be limited, because the non-uniform AM1.5 generation profile requires high collection probability in the p-i interface region as it is intrinsically the case in undoped p-i-n cells after light-soaking (Figure 4). A different situation is encountered in the second cell of a multi-junction cell. This cell is required to convert a more homogenous generation profile, as the high generation peak of the AM1.5 spectrum, due to the strongly absorbed high energy photons, is absorbed in the first cell. In the second cell, a redistribution of the concentrated electric field away from the p-i region towards a more evenly distributed electric field across the entire i-layer offers the potential to improve the degraded state conversion efficiency. To move electric field away from the p-side towards the n-side, the installation of negative space charge is required, i.e. boron doping must be applied.

Our numerical modelling suggests that by graded boron doping the degraded state conversion efficiency of red light could be improved by 20-30 % in a 0.5 μm solar cell. Figure 5 shows the red light JV of a cell with a defect density of $3\cdot10^{16}$ cm^{-3} in the i-layer, and different acceptor densities in the front half of the i-layer: the impurities compensate the positive defect charge at the p-side, and the doped cells show increased degrade state collection efficiency as compared to the undoped cells. The details of the numerical model used in Figure 5 are explained elsewhere [3,11].

Besides the optimal design of the doping profiles in the i-layer, the success of the electric field profiling will critically depend on the extent of additional losses due to the doping itself. It is known that large doping concentrations lead to increased defect densities and therefore to lifetime reductions. The manipulation of the electric fields in a p-i-n solar cell in the proposed way requires only very small doping concentrations, however. Such doping concentrations were found to lead to insignificant changes of defect densities in a-Si:H films [12].

A set of solar cells was prepared with 2 vppm of B_2H_6 doping in the first (zone I), second (zone II), or third (zone III) third of the i-layer. Figure 6 shows the annealed state JV curves for different illumination conditions. Generally, the forward voltage current collection is reduced for all doping cases as compared to the collection in an undoped solar cell. The reduction of the collection is found more pronounced for p-side illumination case (Figure 6 top) than for n-side illumination case (Figure 6 bottom), thus indicating that the collection efficiency has been reduced mostly towards the p-side of the solar cell. This is in agreement with the imposed doping gradient that was designed to shift the electric field

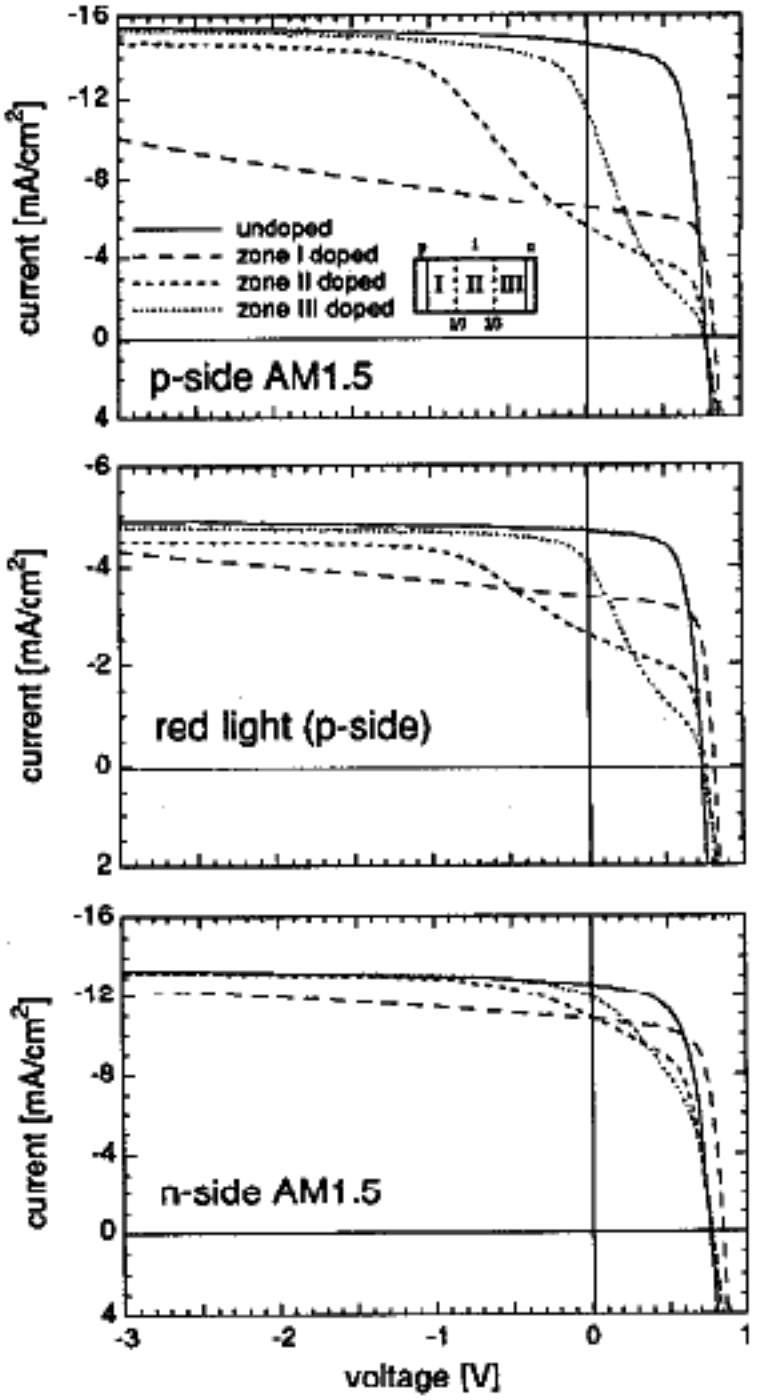

Figure 6: Annealed state JV curves of p-i-n solar cells with different low level graded boron doping in the i-layer: 2 vppm of B_2H_6 was added to the SiH_4 feed gas during the deposition of zone I, II, or III.

towards the n-side. For reverse voltages, the current collection tends to join the (complete) collection of the undoped cell. The fact that at reverse bias voltage all photo-generated carriers can be collected shows that the low-level doped zones have reasonably large photo-carrier lifetimes and are by no means photovoltaicly dead layers as e.g. the highly doped p- and n-layers of a p-i-n solar cell. The pronounced differences found in the current versus voltage curves for the different locations of the boron doping can be understood by considering the details of the electric field propagation in the solar cell i-layer: For low applied voltage (forward), the electric field only extends in the region between the n-layer and the doped zone. With increasing applied voltage (reverse) the acceptors in the low-level doped zone get gradually ionized, until the electric field extends also into the zone between the p-layer and the doped zone.

Figure 7 shows the electric fields at zero applied external voltage as measured by μs current transients from both the p- and the n-side. As electric fields which increase in the direction away from the measurement side can not be measured, the p-

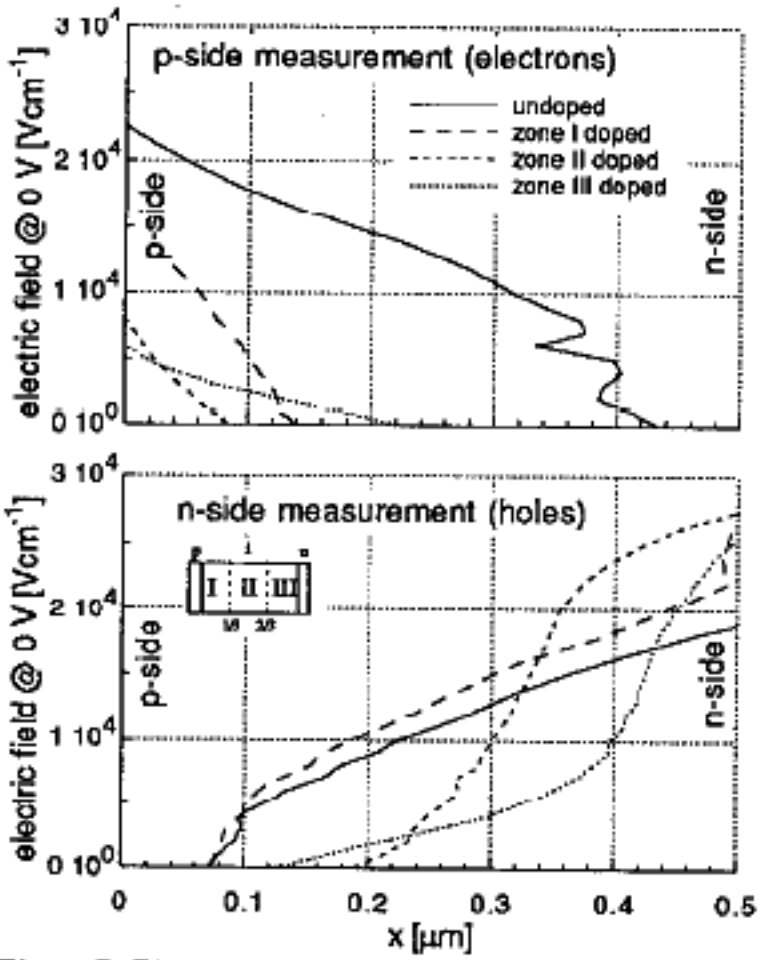

Figure 7: Electric field profiles in graded boron doped p-i-n solar cells as measured from the p- or n-side by µs current transients [5] (doping concentration: 2 vppm B_2H_6)

side measurements only indicate that the boron doped cells have a reduced field at the p-side as compared to the undoped cell. The n-side measurements on the other hand yield detailed information on the electric field distribution. First, all boron doped cells have electric fields higher than the undoped cell closed to the n-i interface. Secondly, the onset of the doping can be detected: For the zone III doped cell, the high field region is limited to the n-i interface region, for the zone II doped cell of the onset of the doping can be seen in the centre of the i-layer, and for the zone I doped cell a relatively small uniform field increase (with respect to the undoped cell) is observed. In summary, the electric field measurements indicate that indeed the electric field is increased in the back of the i-layer by the low level boron doping, with different distribution profiles depending on the doped zone location.

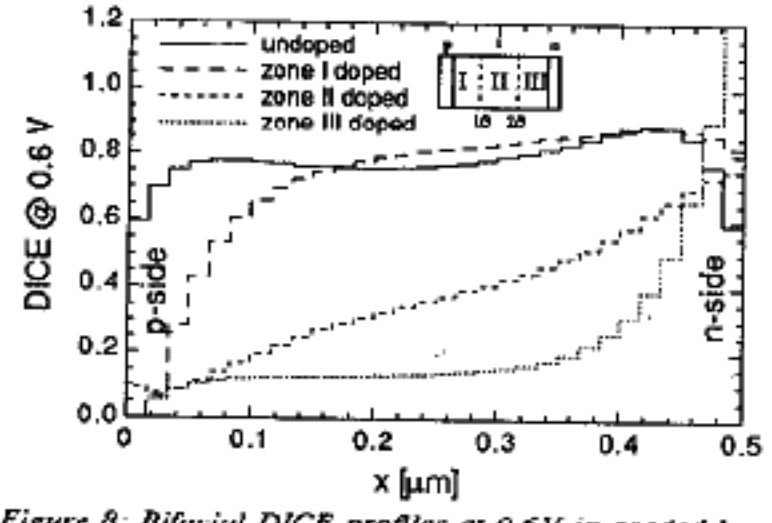

Figure 8: Bifacial DICE profiles at 0.6V in graded boron doped p-i-n solar cells (doping concentration: 2 vppm B_2H_6).

Figure 8 shows the DICE collection probability profiles of the doped cells at +0.6 V applied voltage. The collection profiles at 0.6 V are found to scale with JV data of red light at +0.6 V (Figure 6 middle): whereas for zone I doping collection is high for the whole i-layer except for the region close to the p-i interface, for zone III doping the collection is suppressed over most of the i-layer except the region close to the n-i interface. As red light current collection is proportional to the average collection from the entire i-layer, the current scale with the areas under the DICE profiles of Figure 8.

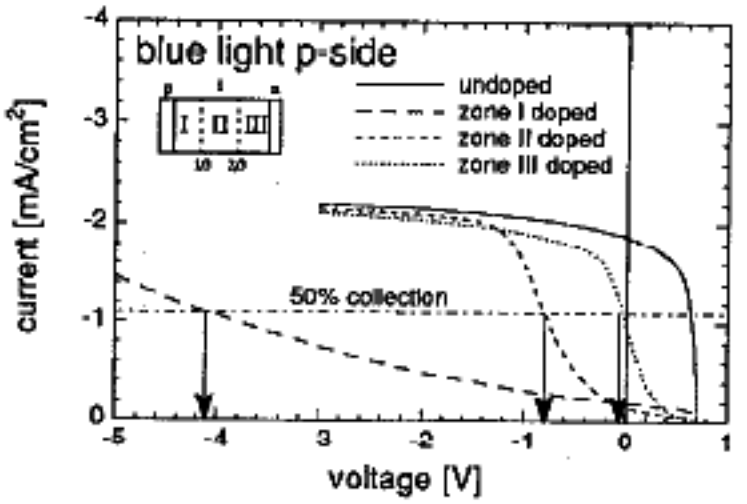

Figure 9: p-side blue light (AM1.5 filtered with BG12 band-pass filter) JV of graded boron doped p-i-n solar cells (doping concentration: 2 vppm B_2H_6).

It was argued above that the detailed shape of the JV curves in the boron doped solar cells is the result of changing electric field propagation in the i-layer. In Figure 9 the propagation of the electric field to the i-layer region on the p-side of the doped zone was directly probed by strongly absorbed light: clearly a critical voltage defines the onset of the collection for each doping location. The critical voltage systematically increases as the doped zone moves towards the p-side. This critical voltage can now be used to quantitatively establish the active dopant concentration (q_B) as follows:

The critical voltage it considered to be that at which the electric field at the p-side of the doped zone, for decreasing reverse voltage, is exactly cancelled. The total integrated dopant charge ($q_B \cdot L/3$) is taken to be concentrated in a single sheet of charge of negligible width at the i-layer position x (see Figure 10). The Poisson's equation can be used to relate the electric field on the left (E_1) and the right (E_2) of the doping charge sheet (e is the elementary charge, ε is the permittivity)

$$E_2 - E_1 = \frac{e}{\varepsilon} \cdot q_B \cdot \frac{L}{3} \qquad (1)$$

Since the integration of the electric field over the whole i-layer must equal the applied potential

$$E_1 \cdot x \cdot L + E_2 \cdot (1-x) \cdot L = V_{ext} + V_{bi} \qquad (2)$$

At the critical voltage $V_{ext} = V_{critical}$ we define

$$E_1 = 0 \qquad (3)$$

By combining (1), (2), and (3), the dopant charge density as a function of x and $V_{critical}$ is

$$q_B = \frac{3}{L^2} \cdot \frac{\varepsilon}{e} \cdot \frac{V_{critical} + V_{bi}}{(1-x)} \qquad (4)$$

In Table III shows the evaluation of the dopant charge density q_B for the three doping cases. The built in potential V_{bi} was assumed to be 1V in all cases. Given the simplicity of the model, the result yields fairly consistent values for the charge

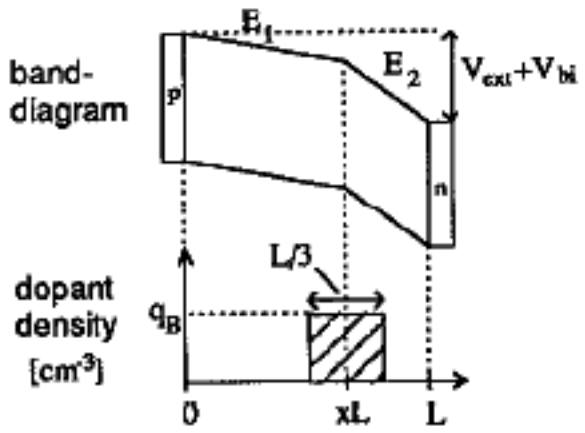

Figure 10: Schematic band-diagram and doping profile of graded boron doped p-i-n solar cells.

density of ~3-4·10^{16}cm^{-3}. The boron concentration in 2 vppm B_2H_6 doped films was also measured by SIMS and found to be of ~3·10^{17}cm^{-3}. From this we can estimate the fraction of active, 4-fold co-ordinated boron dopants to be ~10-15%, similar to values found in the literature.

Table III: Dopant space charge density determined by the p-side blue light collection threshold

doped zone	x	$V_{critical}$ V	$V_{critical}+V_{bi}$ V	q_B cm^{-3}
I	0.17	-4.2	-5.2	$4.7 \cdot 10^{16}$
II	0.5	-1.8	-2.8	$2.8 \cdot 10^{16}$
III	0.83	-0.1	-1.1	$4.5 \cdot 10^{16}$

In summary, the results of the low-level graded boron doping in the i-layer of the solar cells show that the doping yields changes of the electric field as expected. The results can be quantified in terms of electric field distributions to an extent that even allows for quantitative analysis. At a doping concentration of 2 vppm B_2H_6, with a dopant charge density well in the range of the expected degraded state defect concentrations (that are to be compensated), the collection measurement results do not indicate the presence of strongly enhanced recombination in the doped zones.

LIGHT-SOAKING OF THE LOW-LEVEL BORON DOPED SOLAR CELLS

The set of low level doped cells was light-soaked at one sun for 425 hours. During light-soaking, depending on the doping location and the illumination, the boron doped solar cells exhibit increasing solar cell performance. These important recovery effects directly prove the existence of electric field changes induced by the light-induced defects. They result from the creation of defects in the i-layer, which by their positive charging gradually counteract the field shift of the boron doping. P-side efficiency of the zone III doped cell is given as a function of light-soaking time in Figure 11 (see also Figure 13). Similar, however less substantial recovery in boron doped cells has been reported previously [13,14].

The recovery effect in the boron doped solar cells can only be explained in terms of charged light induced defects compensating the charge of the boron atoms in the i-layer. While it was not the principal reason for undertaking this research it is possible to use these observations to address some theoretical aspects of defect generation. In order for the recovery to proceed under light exposure it is necessary for the light to produce dangling bonds in the near interface regions and for these to take on a charge consistent with the majority

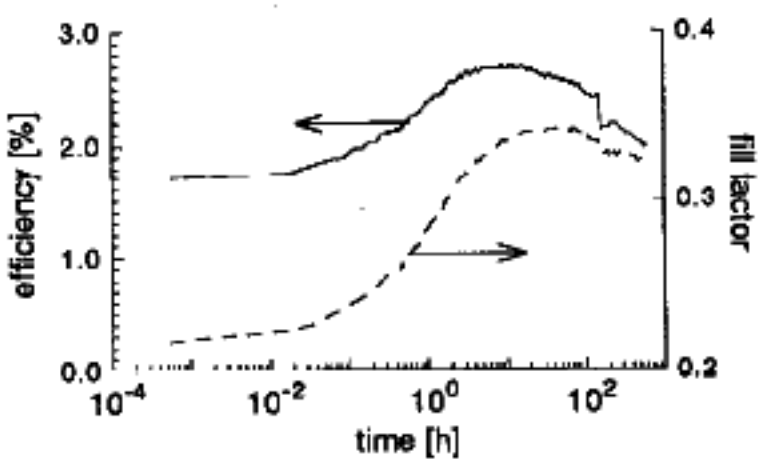

Figure 11: Fill factor and efficiency of a zone III 2 vppm boron doped solar cell monitored during light-soaking under a sodium discharge lamp. The intensity was set to match the short circuit current of 100 mW/cm^2 AM1.5. The illumination is from the p-side.

carrier of the region. Therefore these defects could not be produced by the fermi level position alone (without light) as suggested by some defect creation models [15].

The DICE profile after light-soaking (Figure 12) shows the effectiveness of the field changes induced by the boron doping: In all cases the n-i region collection remains higher than that in the undoped cell. Towards the p-side the collection probabilities increase somewhat as compared to the annealed state, but they generally stay lower than those in the undoped cell.

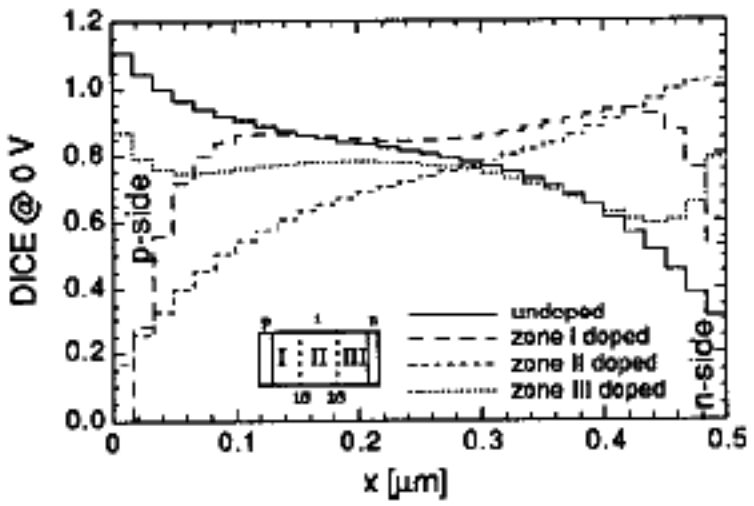

Figure 12: Bifacial DICE spectrum at 0V of graded boron doped p-i-n solar cells after 425 hours of light-soaking (doping concentration: 2 vppm B_2H_6).

Figure 13 shows the efficiency of the boron doped solar cells before and after light-soaking, and for different illumination conditions. The conversion efficiency for p-side AM1.5 illumination is the highest for the undoped cell, in agreement with the DICE profile. The increase of the electric field at the p-side due to the light-soaking was thus not strong enough to obtain a high collection from this region. For n-side AM1.5 illumination, however, all boron doped cells perform better than the undoped cell in the light-soaked state, even cells that in the annealed state showed much lower efficiencies than the undoped cell. This confirms that electric field modification was able to increase the collection from the n-i region in the light-soaked state.

For the crucial red light efficiency that requires high average collection from the entire i-layer, the solar cell with zone I doping is found to have the same efficiency as the undoped cell, whereas the other doped cells perform only

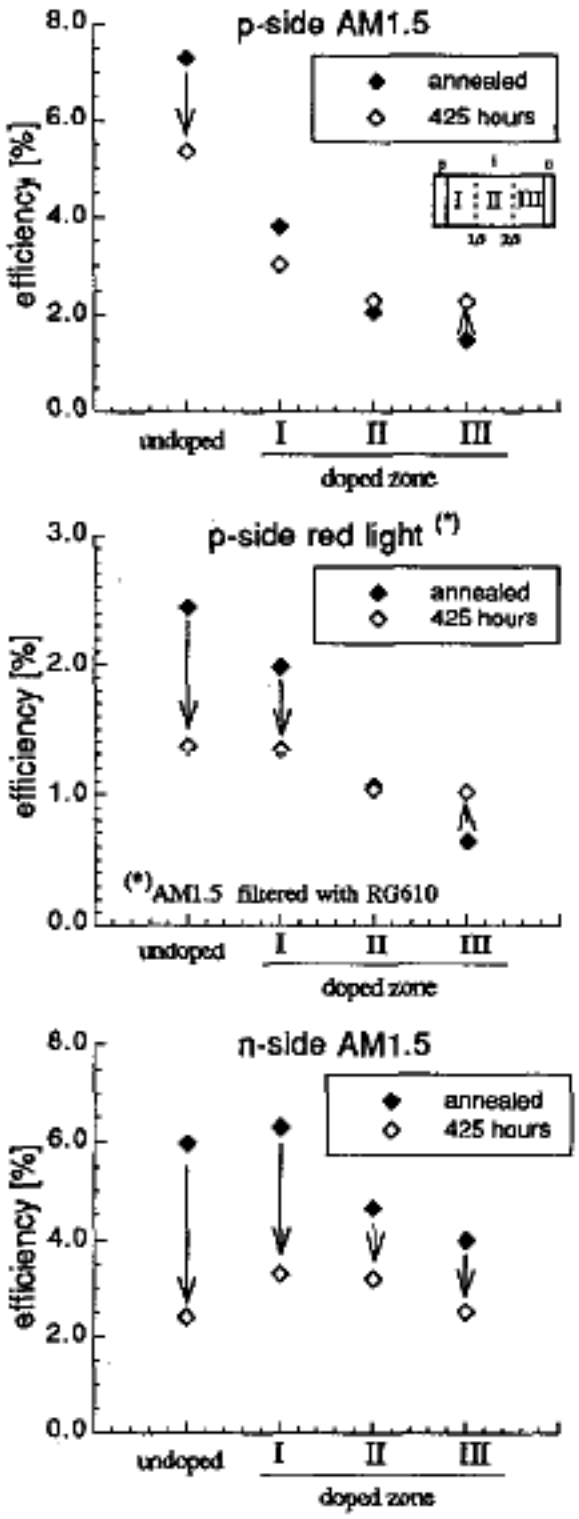

Figure 13: Efficiency of graded boron doped p-i-n solar cells in the annealed state and after 425 hours of light-soaking (doping concentration: 2 vppm B_2H_6).

slightly worse. Clearly, the degraded state red light conversion efficiencies of the boron doped and of the undoped cells are in the same range, which is remarkable considering the large differences in the annealed state, and the fact that the standard cell degraded to this state and some of the boron doped cells increased their efficiency during the light-soaking to obtain the same level of performance. From this, it can be stated that the boron doping in the concentrations used here definitely does not lead to excessively high defect densities when used to modify the electric field distribution in the i-layer of p-i-n cells. Because the doping concentrations in the present set of boron doped cells was exceedingly high (the p-side collection remains to strongly suppressed after light-soaking) and the profiles are crude (uniform in the doped zones) no actual gain in red light conversion was realized. Further doping experiments employing optimized doping profiles should make it possible to reach this goal.

CONCLUSIONS

The monitoring of the degradation of p-i-n solar cells by bifacial measurements shows that in the degraded state the carrier collection is continuously decreasing from the p-side toward the n-side of the i-layer. An asymmetrical field distribution, due to predominately positive charging of the light-induced defects and a resulting high electric field at the p-i interface, can explain this asymmetry.

Improvement of the degraded state performance of p-i-n solar cells seems possible by a directed redistribution of the electric field towards the n-side of the i-layer. Numerical modelling shows that the degraded state conversion of red light can be improved by 20-30 % by graded boron doping. Such an improved solar cell would be a superior second cell of a multi-junction cell.

Bifacial solar cells measurements, including µs current transient measurements, show that by graded i-layer boron doping the electric field distribution in the i-layer can be manipulated in a controlled way. The doping concentrations needed to substantially modify the electric field distributions are found not to induce noticeable excess defects due to the doping of the material itself. Also a novel analysis of the p-side collection threshold yields the density of active dopant charge in the i-layer directly from a solar cell measurement.

If the graded boron doped cells are degraded, recovery of the p-side collection, and more stable n-side efficiencies confirm the mechanisms of field shifts and compensation of defect charge by the doping. Together with red light efficiencies similar to the ones found in undoped cells, this shows the viability of the proposed concept of electric field optimisation.

ACKNOWLEDGEMENTS

The authors wish to thank S. Dubail for the sample preparation, and M. Goetz for carrying out a light-soaking experiment. This work was supported by the Swiss Federal Office of Energy (OFEN) under contract EF-REN 90(045).

REFERENCES

[1]: R. S. Crandall, 21th IEEE PVSC Proc.(1990) p.1630
[2]: H. E. P. Schade, United States Patent, No 4.772.933, Sept. 20, 1988
[3]: D. Fischer et al, 11th European Photovolt.Solar Energy Conf.(1992) p.560
[4]: T. Takahama et al, Jap.J.of Appl.Phys. 23 (1986) p.1538
[5]: R. Vanderhagen, C. Longeau, MRS Symp. Rec 149 (1989) p.357
[6]: N. Wyrsch et al, 11th European Photovolt.Solar Energy Conf.(1992), p.742
[7]: Y. Uchida et al, Solar Cells 9 (1983) p.3
[8]: X. R. Li et al, MRS Symp.Rec.258 (1992) p.929
[9]: K.W. Mitchell, 18th IEEE PVSC Proc.(1985) p.914
[10]: J. Hou et al, 11th European Photovolt.Solar Energy Conf.(1992) p.750
[11]: C. M. Fortmann, D. Fischer, at this conference
[12]: E. Sauvain et al, Solid State Comm., 85, 3 (1993) p.219
[13]: M. Onishi et al, MRS.Symp.Rec.219 (1991) p.421
[14]: D. Fischer et al, MRS Symp.Rec.258 (1992) p.887
[15]: R. Brüggemann et al, MRS Symp.Rec.258 (1992) p.729